Latent Heat Flux over the North Atlantic Ocean—A Case Study

SUSANNE CREWELL,* EBERHARD RUPRECHT, AND CLEMENS SIMMER

Institut für Meereskunde Kiel, Germany

(Manuscript received 9 October 1990, in final form 15 February 1991)

ABSTRACT

Nimbus-7 SMMR data and ship observations are combined to compute the latent heat flux using the bulk aerodynamic method. Sea surface temperature (SST) and the surface humidity are determined with the microwave data. The surface wind field is derived from an analysis of ship observations of wind speed and surface pressure by means of a boundary-layer model by Bumke and Hasse. The microwave-derived SSTs are calibrated against those calculated from Advanced Very High-Resolution Radiometer (AVHRR) data. To get reliable results in the northern parts of the North Atlantic, only ascending (daytime) orbits of *Nimbus-7* were used. Daytime data show a larger bias due to solar heating of the instrument but lack the complicating effects of differential cooling when the satellite enters the earth's shadow at the beginning of the descending orbits.

The evaporation fields are derived over the North Atlantic for individual overpasses of the satellite during July 1983, with a spatial resolution of 1° × 1°. High temporal and spatial gradients are observed, which are consistent with the prevailing synoptic situations. In the area south of Greenland and east of Canada, where the Labrador Current is located, latent heat flux (LE) is negative even in the monthly mean. The reliability of the negative values is demonstrated by a case study. They coincide well with ship observations of fog events.

The flux of latent heat can be determined with an acceptable accuracy of 25–40 W m^{-2} for individual values if the bias of the SMMR data can be reliably removed.

1. Introduction

Evaporation at the ocean surface is an important component of the hydrological cycle. It affects both the ocean and the atmosphere. Together with precipitation, it determines the freshwater flux into the ocean. At the same time, the large amount of energy that is needed for the evaporation is carried upward by the water vapor from the ocean into the atmosphere. This latent heat flux LE is the main energy loss for the oceans [51% of the incoming solar energy is used for evaporation (Dietrich et al. 1975)] and the main energy source for many processes in the atmosphere, particularly in the tropics (cloud cluster and tropical storms). To understand the oceanic and atmospheric circulations and their interconnections, LE must be accurately known. For oceanic climate-related experiments an accuracy of 10 W m^{-2} for regions 500 × 500 km^2 is needed (Taylor 1984).

Evaporation over the oceans cannot be measured directly; it has to be derived from other meteorological–oceanographical parameters. The most accurate methods (correlation, dissipation, and profile method) are also not able to feasibly describe the large-scale evaporation over the ocean, since they need a large experimental effort. Since LE varies strongly in time and space, there is a need for more observations than those methods could provide. With the bulk aerodynamic method (1) (which results from the desire to determine LE from routinely recorded meteorological ship observations that provide the main data source over oceanic areas), it is possible to close the gap.

Here,

$$\mathrm{LE} = LC_E\rho V_{10}(q_s - q_{10}) \quad (\mathrm{W\ m^{-2}}) \qquad (1)$$

with L as the latent heat of vaporization ($m^2\ s^{-2}$), C_E the bulk transfer coefficient for humidity (Dalton number), ρ the density of air (kg m^{-3}), V_{10} the wind speed at a reference level (normally 10 m) (m s^{-1}), q_s the saturation specific humidity at surface temperature (g kg^{-1}), and q_{10} the specific humidity at a reference level (normally 10 g kg^{-1}).

More than 20 different sets of C_E have been published (for a review see Blanc 1985; Isemer 1987; Smith 1989), including stability and wind speed dependence. Most of these dependencies result from theoretical considerations, but up to now, there is hardly an experimental proof. First results from the HEXOS experiment (Heat Exchange over the Sea, see Smith et al. 1990) indicate: $C_E = 1.2 \times 10^{-3}$ without any wind-

* Present address: Institut für Fernerkundung, Universität Bremen, Germany.

Corresponding author address: Dr. E. Ruprecht, Institut für Meereskunde an der Universität Kiel, Düsternbooker Weg 20, D-2300 Kiel, Germany.

speed dependency, at least up to 18 m s^{-1}. Using the equation of state, ρ can be determined from surface air pressure and temperature. The most important factors in the bulk formula are V_{10}, as a measure of the intensity of turbulence and the vertical humidity gradient $q_s - q_{10}$.

Ship observations used in the bulk aerodynamic method are numerous, but their poor quality and uneven distribution (concentration on routine ship routes) allow only the calculation of long-term climatological mean values (e.g., Bunker 1976; Isemer and Hasse 1987). Satellite observations are able to provide parameters used in the bulk parameterization. Passive microwave soundings are most appropriate because the important parameters, SST, V_{10}, and q_{10} can be derived, or at least estimated, under almost all weather conditions. Infrared observations alone are not sufficient because they do not provide wind speeds, and their restriction to cloud-free situations would lead to highly biased results. The near-surface humidity q_{10} cannot be derived directly from satellite remote sensing, but it is possible to relate q_{10} to the total precipitable water W (Liu and Niiler 1984; Liu 1988; Wagner et al. 1990). One disadvantage is the poor information that can be drawn from satellite data about the stability in the marine boundary layer.

Liu (1984) used data from the Seasat SMMR (Scanning Multichannel Microwave Radiometer) for a case study over the North Atlantic. He calculated mean LE over the 92-day Seasat period for 2° × 2° bins. Later (Liu 1988) he applied the bulk method to monthly mean values of V_{10}, q_s, and q_{10} in tropical oceans in the same spatial resolution to study ENSO (El Niño–Southern Oscillation) events. In a comparison with ship data, he determined the error for SMMR-derived LE to be 27 W m^{-2}. For the ship determinations he gave an accuracy of 31 W m^{-2}.

In this study, *Nimbus-7* SMMR data and ship observations are combined and used in the bulk aerodynamic method. AVHRR data are used to calibrate the microwave-derived SST. The aim is to derive evaporation fields over the North Atlantic for time scales as short as possible. This study differs from Liu's approach by the following aspects:

1) Spatial resolution is 1° × 1°.
2) To get results in the northern parts of the North Atlantic as well, ascending orbits of *Nimbus-7* were used instead of descending orbits (see data section).
3) The bulk formula was applied to actual data (not monthly mean values) of the individual parameters to compute actual fields of LE in order to avoid errors due to the nonlinearity of the bulk formula.
4) A high-quality wind field, derived from ship observations of wind speed and surface pressure by means of a boundary-layer model (Bumke and Hasse 1989), was used instead of the low-quality microwave estimates.

2. Data

Data over the North Atlantic of July 1983 were used from *Nimbus-7* SMMR, *NOAA-7* AVHRR, routine ship observations, and radiosonde ascents to determine the geophysical parameters necessary to evaluate the bulk formula.

a. Nimbus-7 SMMR

The SMMR was operated on the polar-orbiting satellite *Nimbus-7* from fall 1978 to summer 1987. Equator crossing took place at local noon (ascending) and midnight (descending) so that the North Atlantic was viewed by the instrument between 1200 and 1600 UTC during ascending tracks and from 0100 to 0500 UTC by descending tracks. Bipolarized brightness temperatures were measured by the instrument at five frequencies (6.6, 10.7, 18, 21, and 37 GHz) every second day. (For detailed information about satellite and sensor see Gloersen and Barath 1977.) The interpolated brightness temperatures of the grid 1 CELL-ALL data tape (NASA 1985), which has a spatial resolution of 156 × 156 km^2, were used. To eliminate erroneous data, the following filter techniques were applied.

1) LAND EFFECTS

Landmasses have a much higher emissivity (0.7–0.9) in the microwave region than ocean surfaces (0.4–0.5) do; therefore, sidelobe effects can significantly increase the brightness temperatures over ocean areas. For this reason, only data from areas that are at least 600 km from the coasts were used.

2) RAIN ELIMINATION

Cloud liquid water has only a small effect on the microwave signal, which can be corrected. Precipitation, however, perturbs the signal to such a degree that the data cannot be used for other purposes. A histogram analysis of the brightness temperature at 37-GHz horizontal polarization T_{37H}, the channel most sensitive to rain, resulted in an upper threshold of 184 K for precipitation-free cases. In addition, we used the rain-elimination procedure of Milman and Wilheit (1985). To screen out rain-contaminated data, the parameter $p = (T_{6.6V} - T_{6.6H})(T_{6.6V} + T_{6.6H})^{-1}$ is allowed to vary only between 0.24 and 0.28. These limits differ slightly from the values assumed by Milman and Wilheit (1985). The tuning of the thresholds is based on the visual inspection of the derived fields of SST and W, and on the comparison with weather charts. The thresholds were set to remove unrealistic results and areas of possible strong convection. The differences of the p thresholds are attributed to changes in the performance of the SMMR instrument. Both algorithms together removed about 10% of the data.

3) CORRECTION FOR INSTRUMENT HEATING

Because of calibration problems, probably caused by solar heating of the instrument, differences exist between daytime (ascending orbits) and nighttime (descending orbits) measurements. Most authors (Wilheit et al. 1984; Milman and Wilheit 1985; Prabhakara et al. 1983; Bernstein and Chelton 1985) prefer the nighttime data because the satellite is in the earth's shadow. The day–night differences are shown in Fig. 1 for the zonally averaged monthly mean of $T_{6.6V}$ that carries most of the information about the variations of the sea surface temperature. At 22°N, $\bar{T}_{6.6V}$ is higher by 4 K for the ascending tracks (daytime) compared to the descending (nighttime) tracks. This corresponds to roughly an 8-K difference in SST. At 62°N the difference is negligible. Moreover, at latitudes north of 50°N, the signal of the nighttime data remains almost constant, while the daytime data further decrease due to the decreasing SST. This decrease in SST is also documented by AVHRR IR estimates for the same month. The result coincides with the findings of other authors. Eymard et al. (1989) derived abnormally high SSTs north of 45°N. Milman and Wilheit (1985) interpreted their high SSTs as an influence by landmasses. We think, however, that this is caused by an increase of the instrument temperature when the satellite crosses the Arctic. At the beginning of the descending orbit the satellite is still illuminated by the sun, especially in summer. When it enters the shadow zone during its southward flight, the satellite cools down and the systematic error of the brightness temperatures slowly diminishes. The reduction of instrument noise and the increase of the SST seem to almost balance each other during the beginning of the southward tracks. During the ascending part of the orbit the satellite is already heated to equilibrium over the South Atlantic. Crossing the North Atlantic, brightness temperatures will have a bias, but the bias is constant over the whole area. Thus, we think data from the ascending orbits are of better quality and should be used. But it must be kept in mind that the observed bias might change with time and that different calibrations must be applied for other months and years. The best correction would be to recalibrate individual channel brightness temperatures. Since no reliable calibration coefficients were available for July 1983 at the time of this study, the derived sea surface temperature and precipitable water were corrected instead.

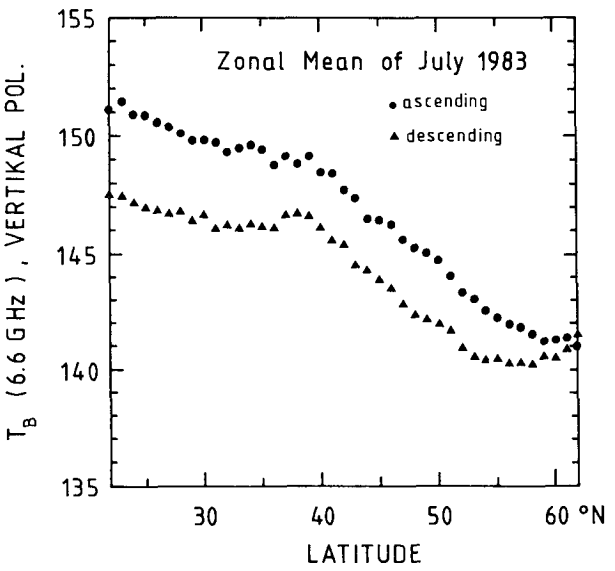

FIG. 1. Zonal and monthly mean of the 6.6-GHz radiation temperature (vertical polarization) for July 1983 from 22° to 62°N over the North Atlantic Ocean.

To determine the SST, the algorithm by Milman and Wilheit (1985, version 2) was selected (without using their correction factors) to compensate for solar-heating effects. For the determination of W, the algorithm by Gloersen et al. (1984) was applied. Their method performed best in a comparison of different algorithms (Wilheit and Chang 1980; Prabhakara et al. 1982; Gloersen et al. 1984; amongst others) when applied to SMMR data of 1979 over the North Atlantic (Schrader 1989).

b. NOAA AVHRR

AVHRR measurements from channels 4 and 5 were used to determine the sea surface temperature with an algorithm by McClain (see Viehoff 1987). The instrument was flown on *NOAA-7*, which crossed the study area (40°–60°N, 20°–50°W) between 1630 and 1700 UTC. Since a pixel has to be cloud-free to provide usable information for the SST determination and cloud cover over the northern ocean was extensive, only data from six days (1, 4, 6, 7, 12, 28) could be analyzed. Even on these days, cloud cover varies between 60% and 80%. Pearce et al. (1989) show, in a comparison of eight algorithms with in situ data, that the algorithm of McClain underestimates SST by 0.3 K and has a random error of 0.7 K.

c. Synoptic surface observations

Operational ship observations from the North Atlantic (250–300 per day) have been used. In a first step, incorrect data were eliminated by an error check (minimum–maximum test). In a second step the SST field was objectively analyzed once a day (1200 UTC), and all observations were eliminated that differed more than 4 K from this daily analyzed SST field. Liu (1984) used a similar method, but he allowed only 2-K differences from the 92-day mean. In this study, a higher variation of the SST was allowed for because of the better spatial and temporal (actual data) resolution that was obtained. The time–space variation of the Gulf Stream, for instance, can create SST variations higher than 2 K on this scale.

d. *Radiosonde data*

Radiosondes are sparse over oceans compared to synoptic reports. But they are mostly obtained from weather and research ships, and show a higher quality. The three weather ships were concentrated in the northeast Atlantic; thus, their observation may not be representative of all situations over the whole North Atlantic. Accuracy of radiosonde-determined precipitable water W is assumed to be 1.3 kg m^{-3} (Hoehne 1980).

3. Determination of the data fields necessary for the evaluation of the bulk formula

To determine the latent heat flux, fields of the necessary parameters (SST, q_{10}, and V_{10}) were derived in a first step. The calculation uses data based on different physical principles and with different time and space resolutions. In addition, datasets have to be combined, the observation times of which differ considerably.

a. *Sea surface temperature*

Sea surface temperatures are ultimately computed from the *Nimbus-7* SMMR data. Satellite IR data and surface observations are used for calibration and quality checks. Such a comparison is not without problems. Satellites measure the electromagnetic radiation emitted by the upper millimeters (microwaves) or even micrometers (IR) of the ocean, while ship measurements (bucket or intake) determine the water temperature T_W in the 1–10-m depth. At nighttime, a cool surface layer may exist with a temperature 0.2–0.5 K lower than the T_W caused by the strongly reduced turbulent energy transports at the ocean surface. During strong insolation and low-wind situations, this gradient can be reversed during daytime, leading to the so-called "afternoon effect" (Katsaros 1980). To determine the saturation humidity at the surface q_s the radiation or skin temperature should be more adequate than T_W because of its direct contact to the atmosphere, but it must be kept in mind that the bulk coefficients were determined using T_W. The different spatial resolutions of the different sensors also have to be taken into account. Ships perform point measurements, while satellite sensors due to their large footprints provide spatial averages over areas with extensions from few kilometers (IR) to tens of kilometers (microwaves). Strong gradients, hence, can cause large differences between ship and satellite measurements.

The microwave-derived SST is representative of an 156 × 156 km^2 area that contains 39 × 39 subareas of IR observations. Due to cloudiness, only 20% of all IR data during July 1983 could be used for comparisons. The differences in time due to the different orbits of the NOAA and *Nimbus-7* satellites also have to be considered. A time gap exists between both measurements, but it never exceeds 5 h. Ship observations are available every 3–6 h. These differences are considered to be negligible over oceans because diurnal changes are normally well below 0.5 K (Pearce et al. 1989).

An evaluation of the quality of the SMMR-derived SST is carried out by computing monthly mean values of the SST derived from SMMR, AVHRR, and ship observations for 1° × 1° areas. Only for monthly means are a large enough number of samples available to perform a statistical analysis. The SMMR estimates are the only ones to cover all 1° × 1° boxes fairly homogeneously with observations; therefore, boxes with unacceptable data coverage by the other data sources were eliminated and reduced the sample number drastically (see Table 1). The standard deviations (rms) between 2 and 4 K are mainly due to principal differences of the different observing systems. The systematic differences can be described by the bias or the (linear) regression between two variables. If these systematic differences are removed either after subtracting the bias or after recalculating microwave SST with a linear regression curve, the random variations remain. The rms of these random variations are shown in the last two columns of Table 1. The random variances are only between 10% and 60% of the total variances; in particular, those between SMMR and AVHRR are drastically reduced. If it is assumed that, in principle, it is possible to remove systematic errors, the numbers in the two columns give an indication of the accuracies

TABLE 1. Comparison of monthly mean sea surface temperatures for 1° × 1° areas over the North Atlantic (July 1983).

		N	r	rms (K)	Bias (K)	rms$_K$ (K)	rms$_R$ (K)
SMMR versus ships	all	1379	0.93	2.33	−1.14	2.03	1.87
	$N_S > 4$	396	0.90	2.38	−1.51	1.83	1.61
AVHRR versus ships	all	482	0.93	3.07	−2.54	1.72	1.64
	$N_{IR} > 40$ and $N_S \geq 2$	215	0.92	2.95	−2.56	1.46	1.40
SMMR versus AVHRR	all	503	0.96	3.59	−3.34	1.30	1.25
	$N_{IR} > 200$	492	0.97	3.55	−3.33	1.25	1.18
	$N_{IR} > 400$	383	0.97	3.51	−3.30	1.19	1.10

N_S = number of ship observations in an 1° × 1° area, N_{IR} = number of AVHRR SSTs in an 1° × 1° area, N = number of data pairs, r = correlation coefficient, rms$_K$ = rms after subtraction of bias, rms$_R$: rms vs regression line.

of SSTs obtained by the different observing methods. With an error partitioning using the last column data of Table 1, the rms error can be estimated for the monthly mean values to 0.55 K for the IR, 0.95 K for the microwaves, and 1.28 for the ship observations. The first value agrees well with the accuracy for the McClain algorithm, which was mentioned earlier.

The small random variation between SMMR- and AVHRR-derived SST led to the conclusion to calibrate the SMMR SST against those derived from AVHRR data. All single microwave footprints of July 1983 over the North Atlantic were used for the calibration. They had to fulfill two assumptions: 1) at least 200 of the 1521 possible AVHRR SSTs must be available, and 2) the rms of the AVHRR-derived SST within the microwave footprint must be less than 0.8 K (i.e., a homogeneous SST distribution within a microwave footprint area). With these data a linear regression was determined, which was applied to correct the SMMR SST:

$$\text{SST (corrected)} = 1.098[\text{SST (microwave)} - 4.419]. \quad (2)$$

Finally, 0.3 K was added to account for the bias of the IR estimates noted by Pearce et al. (1989). The rms differences of the corrected SST and the IR-derived SST is $\sigma_{IR,\mu} = 1.5$ K. It contains errors that are inherent in both methods. Assuming an uncertainty of $\sigma_{IR} = 0.7$ K for the IR SST (Barton et al. 1989; Pearce et al. 1989) and using error partitioning ($\sigma^2_{IR,\mu} = \sigma^2_{IR} + \sigma_\mu{}^2$), the uncertainty of the microwave estimate of the SST is 1.3 K. This is somewhat smaller than the value given by Gloersen (1984), who calculated the error to be 1.5 K. This improvement is attributed to the elimination of bad data (e.g., only ascending orbits). This analysis shows that it is possible to improve the accuracy of actual SST to almost the same value as the monthly means after a thorough correction and recalibration of the first derived product.

It must be mentioned again that data coverage over the Atlantic Ocean is only reasonable for a determination of actual SST fields by microwave observations. But systematic differences have to be subtracted to reach such an accuracy. Thus, it is mandatory to have sufficient independent calibration points.

In this study, the microwave SSTs were calibrated against the IR SSTs for the individual cases. A comparison of the SSTs calculated this way with data from weather ships L and R shows that this correction is successful. The monthly means agree within ±0.1 K.

b. *Specific humidity at 10 m*

The near-surface humidity cannot be directly remotely sensed from satellites. But there exists an intercorrelation with other geophysical quantities accessible by remote sensing. The two most important ones are W and SST. When compared to radiosonde observations of W (31 observation data pairs were found when a temporal and spatial distance of less than 3 h and 100 km, respectively, was applied), a large bias of 16 kg m^{-2} and a rms of 3.3 kg m^{-2} (even after subtracting the bias) exists between the data. Although the bias can be attributed to drifting sensor properties, the large rms might be caused by the inequality of point measurements from the radiosondes and the area estimates from the satellite. Especially at airmass boundaries, large gradients up to several tens of kilograms per square meter over only 100 km exist. Thus, the microwave estimate of W could only be corrected for the bias obtained by the comparison with the radiosonde data. It must be mentioned, however, that all radiosondes that entered the comparison were north of 45°. Thus, the application of this bias to tropical and subtropical regions may lead to systematic errors.

The specific humidity at 10 m is estimated from the calculated values of SST and W using an algorithm by Wagner et al. (1990) that is based on an EOF analysis of the FGGE 1979 dataset for the North Atlantic. This method is similar to a regression analysis but uses the statistical interrelation between the whole vertical profile and the atmospheric variables close to the surface. A comparison of the derived values of q_{10} with collocated ship observations gives an rms of 1.4 g kg^{-1} for individual measurements and 0.8 g kg^{-1} for the monthly mean values. Above 15 g kg^{-1} the algorithm underestimates q_{10} slightly. A cause for this behavior is probably the restricted dataset used for the derivation of the algorithm.

c. *Wind speed at 10 m*

The prevalence of transient synoptic disturbances, especially at the polar front, leads to large spatial and temporal variations in the surface wind field, causing similar fluctuations in the surface flux of latent heat. Microwave measurements have been used to derive the surface wind speed by means of the wind-induced surface roughness, which causes an increase of the surface emissivity and apparent surface temperature. The reliability of these estimates, however, is between 2 and 3 m s^{-1}, especially at low wind speeds (Wilheit et al. 1984). Ship measurements of wind speed also have a large potential to be in error caused by distortion of the wind field by the ship, wrong correction of ship speed, and reading errors, and by mislocation of the ship position. To minimize these errors a 1200 UTC wind field analyzed from all available surface observations of wind speed and surface pressure [prepared by Bumke (1989), private communication] is used employing the method by Bumke and Hasse (1989). Wind and pressure fields are fitted locally by second-order polynomials and are coupled by a boundary-layer model. The spatial resolution of the field is 2° × 2°, and the accuracy is estimated to 1.3 m s^{-1}. The wind

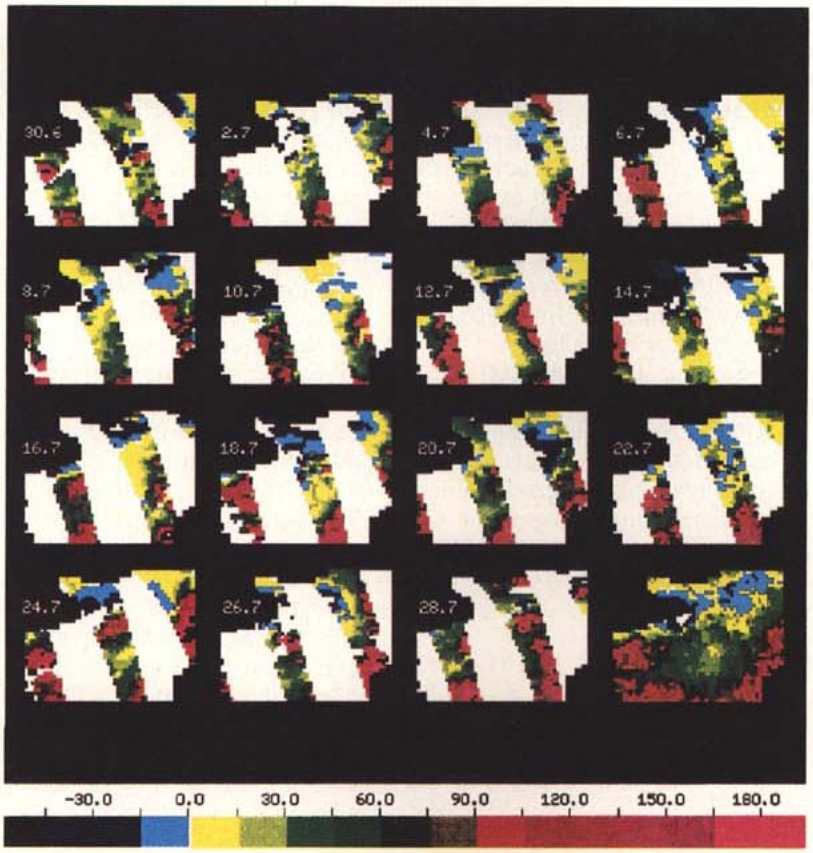

FIG. 2. Flux of latent heat (W m^{-2}) (lower scale) computed from the ascending tracks of *Nimbus-7* SMMR from 30 June to 28 July 1983 for the North Atlantic Ocean (22°–62°N, 15°–69°W) and resulting mean (lower right corner).

field to be used for this analysis is interpolated to a grid of 1° × 1° and is reduced from the analysis height of 25 to 10 m by multiplication with 0.93 (this corresponds to a logarithmic wind profile under neutral stability). Due to the interpolations, the error of this wind field will be slightly higher, but still much better than the ones derived from SMMR.

4. Results

The geophysical parameters described in section 3 were combined to compute the latent heat flux, LE, for all ascending orbits of the *Nimbus-7* SMMR swaths of the period 30 June–28 July 1983 using the bulk formula (Fig. 2). High temporal and spatial gradients are evident. In the area south of Greenland and east of Canada, in the neighborhood of the cold Labrador Current, LE is negative even in the monthly mean. Here the ocean receives latent heat energy from the atmosphere. Stability-dependent bulk coefficients could reduce the magnitude of LE but would not change the negative sign. Even in the long-term climatic mean for July, an area of negative latent heat flux exists, but it is confined to a much smaller area over the central Labrador Current (Isemer and Hasse 1987). This is a preferred region of condensation because dry warm continental air masses are carried over cold water. An actual situation is examined in more detail to study whether the calculated negative values of this study are real. The 12 July results indicate a large area of negative LE reaching from east of Canada to about 45°N, 20°W (Fig. 3). The superimposed surface weather chart for this time shows an anticyclonic region, and the surface ship observations report fog, which is an indication of condensation close to or at the sea surface. The maximum of evaporation in the central North Atlantic fits very well with the cyclonic activity related to the fronts on the surface weather chart.

To evaluate the accuracy of the method, an error propagation can be applied to the bulk formula using the estimated errors of SST, V_{10}, and q_{10} in section 3 (Table 2). This procedure gives an error of the order of 60 W m^{-2} for an actual case, with the assumption that the individual errors are independent from each other. For monthly mean values based on observations every second day, the error would reduce to less than 15 W m^{-2} if it is assumed that the actual data are rep-

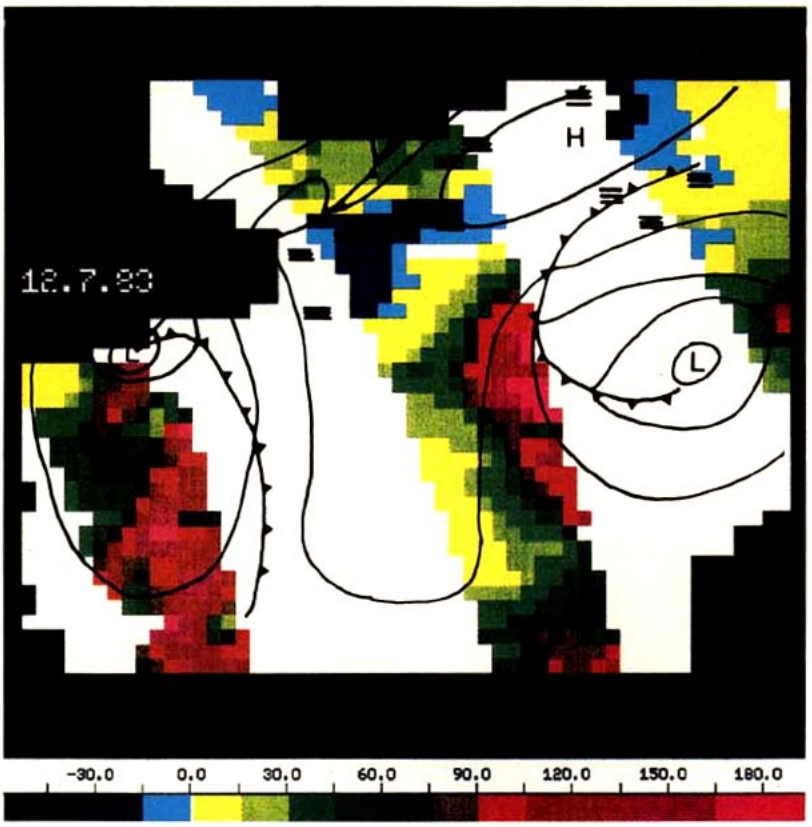

FIG. 3. Flux of latent heat (W m^{-2}) (lower scale) computed from the ascending tracks of *Nimbus-7* SMMR from 12 July 1983. Position of synoptic systems is taken from the 1200 UTC weather chart of the DWD (German Weather Service). The symbol ≡ indicates fog occurrences observed from ships.

resentative of the time period considered. This extrapolation is valid because the narrow swath width of SMMR (about 700 km) combined with the 25° nodal increment of *Nimbus-7* results in measurements almost every fourth day. Compared with a 3-day synoptic time scale the data can be considered independent.

These results are also compared directly to bulk estimates of LE from collocated ship observations (stability dependences were neglected). For the actual cases, the satellite-derived 1° × 1° box estimates were compared to values calculated from ship measurements located in the same box with time gaps less than 3 h. The resulting 216 pairs of observations show a relatively small bias of 13 W m^{-2} (Fig. 4). The few data pairs far off the diagonal (there are also some outside the scale of the plot) are attributed to erroneous ship observations and mislocations, or rain events, which make the microwave-derived data unreliable. The rather high rms of 73 W m^{-2} is mainly caused by the extreme data pairs. Forty-four percent of the data agree better than 20 W m^{-2} and 26% better than 10 W m^{-2}, leading to an rms of 35 W m^{-2} under the assumption of a Gaussian error distribution. If this error is divided equally between ship and satellite estimates, neglecting the sampling errors, the resulting accuracy would be 25 W m^{-2} for individual measurements. It must be kept in mind, however, that the compared values are not completely independent because the wind field used in this method was derived in part from the surface wind observations.

TABLE 2. Error analysis for LE in three climatic locations using error propagation (ΔV_{10} = 1.3 m s^{-1}, ΔSST = 1.3 K, Δq_{10} = 1.4 g kg^{-1}, $L = 2.46 \times 10^6$ m^2 s^{-2}, $C_E = 1.2 \times 10^{-3}$, ρ = 1.23 kg m^{-3}).

Region	V_{10} (m s^{-1})	SST (°C)	q_{10} (g kg^{-1})	LE (W m^{-2})	ΔLE (W m^{-2})	δLE (%)
Midlatitude	10	15	8	94	61	65
Tropics	7	25	16	101	56	55
Condensation	5	10	9	−24	29	120

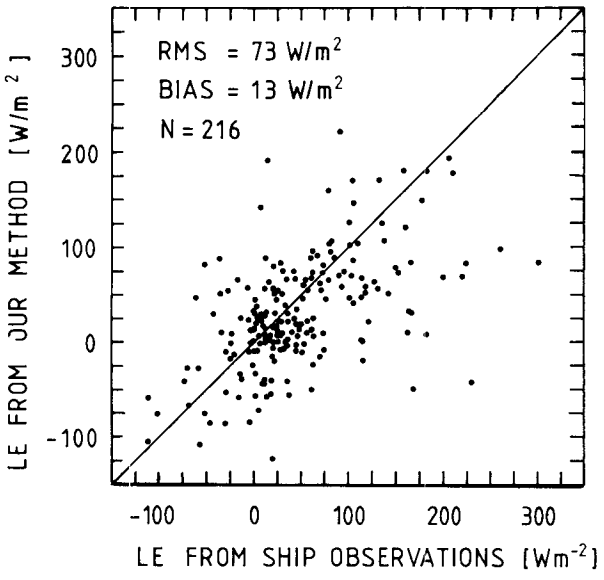

FIG. 4. Flux of latent heat computed from the method for July 1983 compared to values derived from ship observations for individual occasions (diagonal is indicated only).

Monthly mean values of LE were computed from the individual LE estimates and also compared to the monthly means compiled from the ship data (Fig. 5). Full coverage of the area using a 1° × 1° grid is not possible with ship data. Only a few 1° × 1° boxes could be found containing more than ten observations during the month of July. The comparison between these data and the satellite estimates leads to an rms of 39 W m^{-2}. The accuracy of the ship estimates of the monthly mean LE is 29 W m^{-2}. This value was estimated by dividing the ship observations randomly into two groups from which LE was computed individually. Error separation between ship and satellite estimates finally results in an accuracy of the satellite estimates of 26 W m^{-2}. The low density of the ship observations is a major problem in doing this kind of comparison. The adequately filled boxes are all located along the main ship routes. Here the temporal variability is rather high; therefore, the obtained rms of the ship estimates may not be representative for the whole North Atlantic Ocean.

The satellite estimates of the monthly mean are finally compared using the individual method with the so-called climatological method in which monthly mean values of SST, V_{10}, and q_{10} are computed first and then are used to calculate LE. The resulting rms between the monthly means of these two methods is 15 W m^{-2}. It stresses the importance of using the individual method instead of the climatological one.

A few remarks, however, concerning the derived errors are in order. The uncertainties are based on the assumptions that the bulk parameterization of the latent heat flux is correct. In addition, the effect of stability on the bulk coefficient is not taken into account. Both effects will result in higher errors, specifically for the individual estimates. In estimating the error of the monthly mean, the sampling characteristics of the SMMR have not been taken into account. The instrument measures the same spot less than ten times in a month and at the same local time. Although the diurnal cycle may not be that critical over ocean areas, the uncertainties due to the low sampling rate are more serious. The sampling frequency is somewhat lower than the synoptic time scale and may miss major events that largely influence the fluxes of latent heat.

5. Conclusions

The study has shown that it is possible to determine the flux of latent heat LE over the ocean from SMMR and surface data with an acceptable accuracy. The geophysical parameters, which are needed in the bulk formula, are derived with an accuracy of 1.3 m s^{-1} for v_{10}, 1.3 K for SST, and 1.4 g kg^{-1} for q_{10}. This leads to an error of about 60 W m^{-2} for an individual flux with the assumption that the three errors are independent. For a monthly mean (assuming the sampling is optimum in the sense that the derived actual data is representative for the time period of July 1983), the error would reduce to 15 W m^{-2}. If it is assumed that in the near future it is possible to increase the accuracy of the individual parameters to 1 m s^{-1} for v_{10}, 0.5 K for SST, and 1 kg m^{-2} for q_{10}, the error of the flux will reduce to 40 W m^{-2} for individual cases and to 10 W m^{-2} for monthly means. These numbers, however, give the maximum errors (independence is assumed). Our calculations show that, with the accuracy of the geophysical parameters today, the latent heat flux can

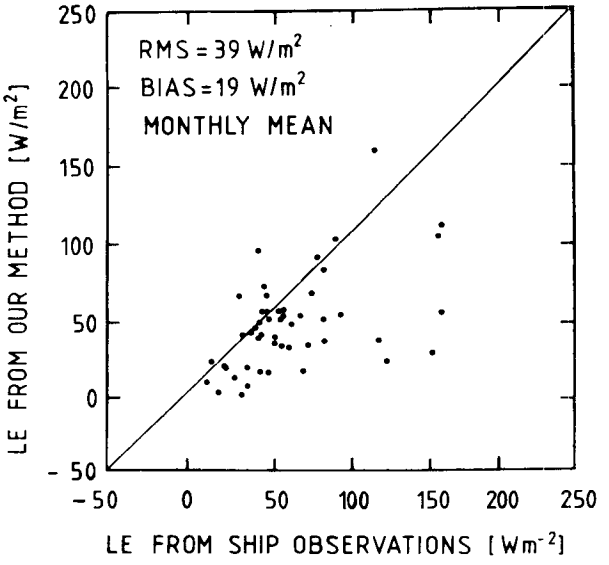

FIG. 5. Monthly mean flux of latent heat (July 1983) computed from this study's method compared to values derived from ship observations for the North Atlantic Ocean (diagonal is indicated only).

be determined with an accuracy of better than 25 W m^{-2} for 1° × 1° boxes at individual times and better than 10 W m^{-2} for monthly means.

These accuracies are possible only if the parameters derived from the microwave observations can be recalibrated by other data (e.g., IR observations or ship data). Such a support is essential as long as reliable on-board calibrations are not available. The largest problems were caused by the strongly biased SMMR radiation temperatures. The use of only daytime measurements of the instrument provided good results, especially in the northern parts of the North Atlantic. Because the instrument was operated from fall 1979 to summer 1987 the SMMR offers the chance to study latent heat variations for almost a decade. This study also urges careful recalibration, especially for the daytime data.

Acknowledgments. The work was supported by the Deutsche Forschungsgemeinschaft (SFB133-B6). Radiosonde and ship observations were provided by the Deutscher Wetterdienst.

REFERENCES

Barton, I. J., A. M. Zavody, M. D. O'Brian, D. R. Cutten, R. W. Saunders, and D. T. Llewellyn-Jones, 1989: Theoretical algorithms for satellite derived sea surface temperatures. *J. Geophys. Res.*, **94**(D3), 3365–3375.

Bernstein, R. L., and D. B. Chelton, 1985: Large-scale sea surface temperature variability from satellite and shipboard measurements. *J. Geophys. Res.*, **90**(C6), 11 619–11 630.

Blanc, T. V., 1985: Variation of bulk-derived surface flux, stability, and roughness due to the use of different transfer coefficient schemes. *J. Phys. Oceanogr.*, **15**, 659–669.

Bumke, K., and L. Hasse, 1989: An analysis scheme for determination of true surface winds at sea from ship synoptic wind and pressure observations. *Bound.-Layer Meteor.*, **47**, 295–308.

Bunker, A. F., 1976: Computations of surface energy flux and annual air–sea interaction cycles of the North Atlantic Ocean. *Mon. Wea. Rev.*, **104**, 1122–1140.

Dietrich, G., K. Kalle, W. Krauss, and G. Siedler, 1975: *Allgemeine Meereskunde, eine Einfuehrung in die Ozeanographie.* Gebr. Bornträger, 593 pp.

Eymard, L., C. Klapisz, and R. Bernard, 1989: Comparison between *Nimbus-7* SMMR and ECMWF model analyses: The problem of the surface heat flux. *J. Atmos. Oceanic Technol.*, **6**, 866–881.

Gloersen, P., 1984: Sea surface temperatures from *Nimbus-7* SMMR radiances. *J. Climate Appl. Meteor.*, **23**, 336–340.

——, and F. T. Barath, 1977: A Scanning Multichannel Microwave Radiometer for *Nimbus-G* and *Seasat-A. IEEE Trans. Ocean. Eng.*, **OE-2**, 172–178.

——, D. J. Cavalieri, A. T. C. Chang, T. T. Wilheit, W. J. Campbell, O. M. Johannessen, K. B. Katsaros, K. F. Kunzi, D. B. Ross, D. Staelin, E. P. L. Windsor, F. T. Barath, and P. Gudmansen, 1984: A summary of results from the first *Nimbus-7* SMMR observations. *J. Geophys. Res.*, **89**(D4), 5335–5344.

Hoehne, W., 1980: Precision of National Weather Service upper-air measurements. NOAA *Tech.* Memo., TM NWST&ED-16, 23 pp.

Isemer, H.-J., 1987: Optimierte Parametrisierungen der klimatologischen Energie- und Impulsfluesse an der Oberflaeche des Nordatlantiks. *Ber. Inst. Meeresk. Kiel*, **160**, 184 pp.

——, and L. Hasse, 1987: The Bunker Climate Atlas of the North Atlantic Ocean, Vol. 1. Observations. Vol. 2. *Air–Sea Interaction*, Springer-Verlag, 570 pp.

Katsaros, K. B., 1980: Radiative sensing of sea surface temperature. *Air–Sea Interaction, Instruments, and Methods*, F. Dobsen, L. Hasse, and R. Davies, Eds., Plenum Press, 293–317.

Liu, W. T., 1984: Estimation of latent heat flux with Seasat SMMR, a case study in the North Atlantic. *Large Scale Oceanographic Experiments and Satellites*, C. Gautier, and M. Fieux, Eds., D. Reidel Publishing, 205–221.

——, 1988: Moisture and latent heat flux variabilities in the tropical Pacific derived from satellite data. *J. Geophys. Res.*, **93**(C6), 6749–6760.

——, and P. P. Niller, 1984: Determination of monthly mean humidity in the atmospheric surface layer over oceans from satellite data. *J. Phys. Oceanogr.*, **14**, 1451–1457.

Milman, A. S., and T. T. Wilheit, 1985: Sea surface temperatures from the Scanning Multichannel Microwave Radiometer on *Nimbus-7*. *J. Geophys. Res.*, **90**(C6), 11 631–11 641.

NASA, 1985: *Nimbus-7* Scanning Multichannel Microwave Radiometer (SMMR), CELL-ALL-TAPE user's guide. NASA Goddard Space Flight Center, Greenbelt, Maryland, Doc. Nr. SASC-T-5-5100-0004-011-84, 62 pp.

Pearce, A. F., A. J. Prata, and C. R. Manning, 1989: Comparison of NOAA/AVHRR-2 sea surface temperatures with surface measurements in coastal waters. *Int. J. Remote Sens.*, **10**, 37–52.

Prabhakara, C., H. D. Chang, and A. T. C. Chang, 1982: Remote sensing of precipitable water over the oceans from *Nimbus-7* microwave measurements. *J. Appl. Meteor.*, **21**, 59–68.

——, I. Wang, A. T. C. Chang, and P. Gloersen, 1983: A statistical examination of *Nimbus-7* SMMR data and remote sensing of sea surface temperature, liquid water content in the atmosphere and surface wind speed. *J. Climate Appl. Meteor.*, **22**, 2023–2037.

Schrader, M., 1989: *Bestimmung des Gesamtwasserdampfgehalts aus Mikrowellenbeobachtungen vom Satelliten aus.* Diplomarbeit an der Universitaet Kiel, 92 pp.

Smith, S. D., 1989: Water vapor flux at the sea surface. *Bound.-Layer Meteor.*, **47**, 277–293.

——, K. B. Katsaros, W. A. Oost, and P. G. Mestayer, 1990: Two major experiments in the Humidity Exchange over the Sea (HEXOS) program. *Bull. Amer. Meteor. Soc.*, **71**, 161–172.

Taylor, P. K., 1984: The determination of surface fluxes of heat and water by satellite microwave radiometry and in situ measurements. *Large Scale Oceanographic Experiments and Satellites*, C. Gautier and M. Fieux, eds., 223–246.

Viehoff, T., 1987: Bestimmung mesoskaliger Variabilitaeten der Oberflaechentemperatur und der Attenuation im Nordatlantik aus Satellitenmessungen. *Ber. Inst. Meeresk. Kiel*, **162**, 192 pp.

Wagner, D., E. Ruprecht, and C. Simmer, 1990: A combination of microwave observations from satellites and an EOF analysis to derive vertical humidity profiles over the ocean. *J. Appl. Meteor.*, **29**, 1142–1157.

Wilheit, T. T., and A. T. C. Chang, 1980: An algorithm for retrieval of ocean surface and atmospheric parameters from the observations of the Scanning Multichannel Microwave Radiometer. *Radio Sci.*, **15**, 525–544.

——, J. R. Graeves, J. A. Gatlin, D. Han, B. M. Krupp, A. S. Milman, and E. S. Chang, 1984: Retrieval of ocean surface parameters from the Scanning Multifrequency Microwave Radiometer (SMMR) on the *Nimbus-7* satellite. *IEEE Trans. Geosci. Remote Sens.*, **GE-22**, 133–143.